ELECTROHYDRODYNAMIC INDUCTION PUMPING IN A CLOSED CONDUIT

by

MILLARD SHERWOOD FIREBAUGH

M.I.T. May, 1966

ELECTROHYDRODYNAMIC INDUCTION PUMPING IN A CLOSED CONDUIT

by

Millard Sherwood Firebaugh

S.B., Massachusetts Institute of Technology
1961

SUBMITTED IN PARTIAL FULFILLMENT OF THE

REQUIREMENTS FOR THE DEGREES OF

MASTER OF SCIENCE

AND

NAVAL ENGINEER

at the

Massachusetts Institute of Technology
June, 1966

ELECTROHYDRODYNAMIC INDUCTION PUMPING

IN A CLOSED CONDUIT

by

Millard Sherwood Firebaugh

Submitted to the Department of Naval Architecture and Marine Engineering and to the Department of Electrical Engineering on May 20, 1966 in partial fulfillment of the requirements for the degree of Master of Science and Naval Engineer.

ABSTRACT

An electrohydrodynamic traveling wave induction interaction with the bulk of a slightly conducting liquid (conductivity of approximately 10^{-10} mhos/meter) is shown to produce a fluid flow. A gradient in conductivity normal to the direction of flow is required. In the scheme described here the conductivity gradient is provided by taking advantage of the temperature dependence of conductivity. A traveling potential wave is created on an arrangement of electrodes parallel to the flow direction and in contact with the liquid. The resulting fields induce charges in the bulk which lag the traveling potential wave. Therefore, a time-average electric traction in the bulk is created, motivating the liquid. Expressions for the fields, the time-average traction, and the fluid velocity are derived and discussed. Experimental results are shown which lend credence to the derived equations.

Thesis Supervisor: James R. Melcher
Title: Assistant Professor of Electrical Engineering

ACKNOWLEDGEMENT

The author wishes to thank Professor James R. Melcher for the constant influx of ideas and assistance which he gave so freely during the work of this thesis, which resulted from his earlier work in the same area.

Thanks are also due to Mr. Paul Warren and Mr. Edmund Devitt for their suggestions and assistance, and to Miss Carol Cook for her patience and concern while typing this thesis.

This research was carried out under NASA Grant No. NsG 368.

TABLE OF CONTENTS

TABLE OF CONTENTS
(cont)

CHAPTER I

INTRODUCTION

Induced charges in a slightly conducting liquid can interact with traveling wave electric fields to produce a fluid flow. One method of producing this kind of electroconvection is to introduce a potential wave traveling parallel to an air liquid interface. Induced charges in the liquid will relax to the interface and form a traveling wave of surface charge which will lag behind the potential wave. An electric surface shear will result and the liquid will move.* In this kind of device the interface is a singular point in a gradient of conductivity.

An extension of the concept of the surface interaction would be to produce a continuous gradient in conductivity in a liquid. Then eliminate the interface by bringing the electrodes carrying the traveling potential wave into contact with the liquid. Charges induced in the liquid will no longer relax to the surface but will remain in the bulk of the liquid. A kind of internal wave of induced charge will then travel along behind the traveling potential wave and the possibility for an electric traction in the bulk of the liquid is created.

This phenomenon is very dependent on the charge relaxation time which is the ratio of permittivity to conductivity. If the charge

---

*Melcher, J.R., "Traveling Wave Induced Electroconvection" to be published in Physics of Fluids.

relaxation time for the liquid is very short, then charge will be induced in the liquid but will relax so quickly that it will not lag behind the traveling potential wave. On the other hand, if the relaxation time is very long, then very little charge will be induced in the material and the interaction with the traveling field will be negligible.

EHD induction pumping would be feasible for a wide class of liquids whose relaxation times would be compatible with reasonable frequencies for which traveling electric potential waves might be generated.

In succeeding chapters, a theory and experiment will be described which deal with the phenomenon of electrohydrodynamic pumping of liquids in the bulk. The results obtained are somewhat surprising.

CHAPTER II

THEORY

A. Introduction

The basis of the following theory for electrohydrodynamic induction pumping in the bulk of a slightly conducting liquid is that the movement of charge in the liquid may be explained by a pure conduction model. This model applied to induction pumping in the bulk results in currents which are small enough that the problem may be considered to be only an electric problem and magnetic effects may be ignored. The theory as developed here leads to a conclusion which at first glance is somewhat startling and violates an intuitive conception of how an induction device ought to operate.

B. Electrical Theory

1. Electric Field Equations

Considering magnetic effects to be small we may immediately write Maxwell's equations in the bulk of the liquid*. They are:

$$\nabla \times \vec{E} = 0 \qquad (1)$$

$$\nabla \cdot \epsilon\vec{E} = q \qquad (2)$$

*Fano, Chu, Adler, Electromagnetic Fields, Energy, and Forces, p.179.

where q is the free charge, ϵ is the permittivity and $\bar{E}$ is the electric field vector. To satisfy conservation of charge

$$\nabla \cdot \bar{J} + \frac{\partial q}{\partial t} = 0 \qquad (3)$$

The free current $\bar{J}$ results from Ohm's Law conduction which written in the coordinate system fixed to the laboratory will be

$$\bar{J} = \sigma \bar{E} + q\bar{v} \qquad (4)$$

where σ is the electrical conductivity and $\bar{v}$ is the velocity in the fluid flow. Since the Electric Reynolds number given by the formula $Re = \epsilon v/\sigma d$ is small for the problem under consideration ($Re \approx 2.6 \times 10^{-2}$) the $q\bar{v}$ term in Equ. (4) may be ignored leading to

$$\bar{J} = \sigma \bar{E} \qquad (5)$$

Equation (1) allows that $\bar{E}$ may be written as the negative gradient of the potential Φ.

$$\bar{E} = -\nabla \Phi \qquad (6)$$

Combining Equs. (2), (3) and (6) leads to:

$$\nabla \cdot (\sigma \nabla \Phi) + \frac{\partial}{\partial t} (\nabla \cdot (\epsilon \nabla \Phi)) = 0 \qquad (7)$$

If both σ and ϵ are functions of y in the coordinate system shown in Fig. 1, this equation is in general difficult to solve, however, there are situations in which it may be easily approached.

One such case occurs if it is assumed that ϵ is a constant throughout the bulk of the liquid and that σ may be represented as:

$$\sigma = \sigma_o + \sigma_1 (\zeta - \zeta_o) \tag{8}$$

where ζ is the normalized depth in the channel. $\zeta = y/d$. ζ_o represents some appropriate depth in the channel where a value of σ is measured which is in some sense an average value of conductivity in the channel. It is also necessary that the values of σ_1 and σ_o be such that it is reasonable to say that $\sigma \approx \sigma_o$ in the liquid but $\nabla \sigma = -i_y \sigma_1/d$, where $-i_y$ is the unit vector in the y direction.

Combining equations (8) and (7) with ϵ a constant leads then to:

$$\sigma_o \nabla^2 \Phi + \frac{-i_y}{} \frac{\sigma_1}{d} \cdot \nabla \Phi + \epsilon \frac{\partial}{\partial t} (\nabla^2 \Phi) = 0 \tag{9}$$

This equation will now be solved for the two-dimensional case.

2. Traveling Wave Solutions

If the upper surface of the channel is excited with a traveling potential wave of the form:

$$V = \mathrm{Re}\, \hat{V}_o e^{j(\omega t - kx)} \tag{10}$$

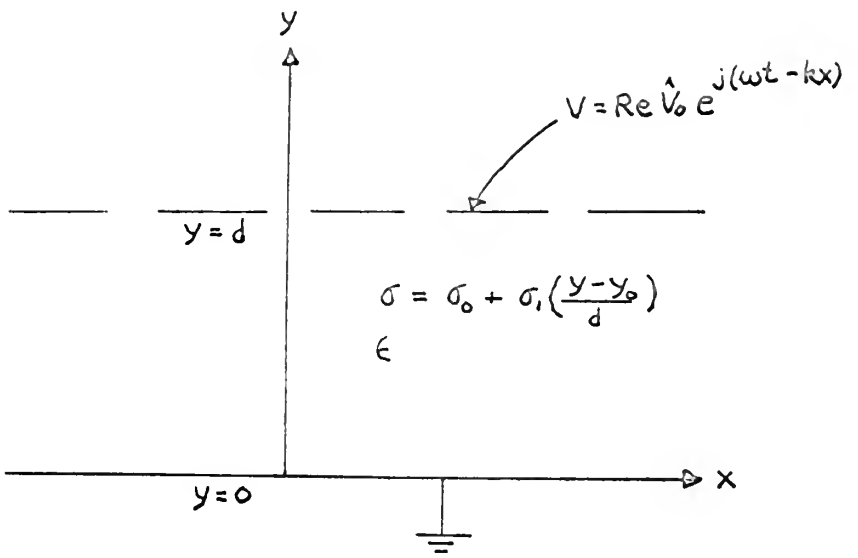

Figure 1 Coordinate system in the pumping channel

where V is the magnitude of the applied voltage, ω is the angular frequency, k is the wave number, and circumflex $\hat{}$ indicates a complex quantity; then the assumed form of the solution of Equ. (9) is:

$$\Phi = \mathrm{Re}\ \hat{\Phi}(\zeta)\, e^{j(\omega t - kx)} \tag{11}$$

Substituting Equ. (11) into (9) gives:

$$\frac{\partial^2 \hat{\Phi}}{\partial \zeta^2} + \frac{\sigma_1}{\sigma_o + j\omega\varepsilon} \frac{\partial \hat{\Phi}}{\partial \zeta} - (dk)^2 \hat{\Phi} = 0 \tag{12}$$

This equation may be solved by assuming for $\hat{\Phi}$ solution of the form $\hat{A}e^{p\zeta}$. Substituting this solution into Equ. (12) and solving for the roots gives:

$$p = \tfrac{1}{2}\left[-\frac{\sigma_1}{\sigma_o + j\omega\varepsilon} \pm \sqrt{\left(\frac{\sigma_1}{\sigma_o + j\omega\varepsilon}\right)^2 + 4(dk)^2}\right] \tag{13}$$

Since in the experiment performed in Chapter IV, $4(dk)^2 \ll (\sigma_1/(\sigma_o + j\omega\varepsilon))^2$ this square root may be expanded around the first term. At the same time defining new constants $\eta = \sigma_1/\sigma_o$ and $S = \omega\varepsilon/\sigma_o$ the roots may be rewritten:

$$p_{\frac{1}{2}} = \tfrac{1}{2}\left[-\frac{\eta}{1 + jS} \pm \left(\frac{\eta}{1 + jS} + \frac{4(dk)^2(1 + jS)}{\eta}\right)\right] \tag{14}$$

Now the complete solution for $\hat{\Phi}$ may be written and the boundary condition on the electric field in the channel may be applied to evaluate the constants of integration:

$$\hat{\Phi}(\zeta) = A_1 e^{p_1 \zeta} + A_2 e^{p_2 \zeta} \tag{15}$$

At the perfectly conducting bottom of the channel where $\zeta = 0$, the appropriate boundary condition is that the tangential component of electric field must be zero. Therefore, $-\partial\Phi/\partial x = 0$ which says that $A_1 = -A_2$. At the top of the channel where $\zeta = 1$ the condition is that $\Phi = V$. This condition says that:

$$A_1 = \frac{\hat{V}_o}{e^{p_1} - e^{p_2}}$$

The final form of Φ is:

$$\Phi = \frac{\mathrm{Re}\, \hat{V}_o (e^{p_1 \zeta} - e^{p_2 \zeta})}{e^{p_1} - e^{p_2}} \; e^{j(\omega t - kx)} \tag{16}$$

Since $E_x = -\partial\Phi/\partial x$ and $E_y = -\partial\Phi/d\partial\zeta$, writing E_x and E_y in the form:

$$E_x = \mathrm{Re}\, \hat{E}_x e^{j(\omega t - kx)} \quad ; \quad E_y = \mathrm{Re}\, \hat{E}_y e^{j(\omega t - kx)}$$

leads to:

$$\hat{E}_x = \frac{jk\,\hat{V}_o(e^{p_1\zeta} - e^{p_2\zeta})}{(e^{p_1} - e^{p_2})} \tag{17}$$

$$\hat{E}_y = \frac{-\hat{V}_o}{d}\frac{(p_1 e^{p_1\zeta} - p_2 e^{p_2\zeta})}{(e^{p_1} - e^{p_2})} \tag{18}$$

Equs. (17) and (18) complete the solution of the electric field problem for the fields in the bulk of the liquid.

C. Fluid Theory

1. Force Equation

The force equation will be written for a two-dimensional flow in a re-entrant channel under the influence of an internal electric shear force which is constant in the x-direction because only the time-average value of the electric stress is considered. The liquid is incompressible and the flow is steady.

The general force euqation is:

$$\rho\left(\frac{\partial \bar{v}}{\partial t} + (\bar{v}\cdot\nabla)\,\bar{v}\right) + \nabla \underline{P} = \nabla\cdot\bar{\bar{T}}_{ij} - \rho g\,\underline{\underline{i_y}} \tag{19}$$

P is the pressure, $\bar{v}$ the flow velocity, ρ the density, and g is the gravitational acceleration. T_{ij} is the total stress tensor

which includes both the electric stress and the viscous stress.

Under the condition described above, the term $\rho(\partial\bar{v}/\partial t + (\bar{v} \cdot \nabla)\bar{v}) = 0$ and Equ. (19) may be re-written as:

$$\frac{\partial P}{\partial x} = \frac{\partial T_{xx}}{\partial x} + \frac{\partial T_{xy}}{\partial y} \tag{20}$$

$$\frac{\partial P}{\partial y} = \frac{\partial T_{yx}}{\partial x} + \frac{\partial T_{yy}}{\partial y} - pg \tag{21}$$

The total stress $T_{ij} = T_{ij}^{E} + T_{ij}^{V}$. The electric stress $T_{ij}^{E} = \epsilon E_i E_j - \frac{1}{2}\delta_{ij}\,\epsilon\, E_k E_k$* and the viscous stress $T_{ij} = \mu\,(\partial v_i/\partial x_j + \partial v_j/\partial x_i)$, where μ may be a function of space.** Substituting these expressions into Equ. (20) leads to:

$$\frac{\partial P}{\partial x} = \frac{\epsilon}{2}\,\partial\frac{(E_x E_x)}{\partial x} + \mu\,\frac{\partial v_x}{\partial x} + \epsilon\,\frac{\partial(E_x E_y)}{\partial y} + \mu\left(\frac{\partial v_x}{\partial y} + \frac{\partial v_y}{\partial x}\right) \tag{22}$$

In the re-entrant channel there can be no gradient in the x direction in pressure. All of the derivatives with respect to x in Equ. (22) are zero because if we consider only time average electric stresses, then all of the stresses in the liquid are constant in the x direction. This leaves only the last two terms

---

* Woodson and Melcher, Fields, Forces and Motions, Ch. 5, p. 35.

** Chandrasekhar, Hydrodynamic and Hydromagnetic Stability, p.12.

of Equ. (22) which is the same as saying:

$$\frac{\partial T_{xy}}{\partial y} = 0 \tag{23}$$

which may be immediately integrated to give:

$$T_{xy} = C_1 \tag{24}$$

where C_1 is the arbitrary constant of integration.

Equ. (21) will not be treated since it is only concerned with the balance of electric forces and gravitational forces in the liquid. This equation concerns the internal instabilities in the flow but does not effect the flow in the x direction, at least in the approximations of this theory.

The time average of the electric stress, which has heretofore only been alluded to, will now be introduced, resulting in the following equation:

$$\frac{\mu(\zeta)}{d} \frac{\partial v_x}{\partial \zeta} = -\frac{\epsilon}{2} \left[\mathrm{Re}\, \hat{E}_x \hat{E}_y^* \right] + C_1 \tag{25}$$

The pulsating double frequency term which results when multiplying two sinusoids has been ignored.

2. Computation of Time-Average Electric Stress

Certain algebraic tricks will be used in this section to perform some computations which are essentially quite tedious. The roots p_1 and p_2 given by Equ. (14) may be rewritten as:

$$\frac{p_1}{2} = \frac{1}{2}\left[-a \pm jb \right] \tag{26}$$

where $a = a_r + ja_i = \eta / (1 + jS)$

and $b = b_r + jb_i = \eta / (1 + jS) + 4(dk)^2 (1 + jS)/ \eta$

From Equs. (17) and (18) it is possible to write that:

$$\mathrm{Re}\, \hat{E}_x \hat{E}_y^* = - \frac{\mathrm{Re} jk \hat{V}_o \hat{V}_o^* (e^{p_1\zeta} - e^{p_2\zeta})(p_1^* e^{p_1^*\zeta} - p_2^* e^{p_2^*\zeta})}{(e^{p_1} - e^{p_2})\ (e^{p_1^*} - e^{p_2^*})} \tag{27}$$

where the asterisk indicates the operation of taking the complex conjugate.

Consider now a term such as $e^{p_1} - e^{p_2}$. Re-writing after substitution for the p's from Equ. (26) leads to:

$$e^{p_1} - e^{p_2} = 2e^{-a/2} \sinh b/2$$

Now $\sinh b/2 = \sinh (b_r/2 + jb_i/2)$ which may be expanded by double angle formulas leading finally to:

$$e^{p_1} - e^{p_2} = 2e^{-a/2}\left(\sinh \frac{b_r}{2} \cos \frac{b_i}{2} + j \cosh \frac{b_r}{2} \sin \frac{b_i}{2}\right)$$

By manipulative tricks of this sort with which the reader may not wish to be bored it is possible to reduce Equ. (27), not, however, without some effort, to the following form:

$$\mathrm{Re}\ \hat{E}_x \hat{E}_y^* = \frac{kV_o^2 e^{-a_r(\zeta-1)}\left[b_r \sin b_i\zeta - b_i \sinh b_r\zeta + a_i(\cosh b_r\zeta - \cos b_i\zeta)\right]}{2d\,(\cosh b_r - \cos b_i)} \qquad (28)$$

The values of the a's and b's may now be computed by combining Equ. (14) with Equ. (26). In the experiment described in Chapter IV, it turns out that $\eta / (1 + S^2) \gg (dk)^2/\eta$. Ignoring the term on the right side of this inequality in the expressions for the p's results in the following values for the a's and the b's:

$$a_r = b_r = \eta/(1 + S^2) \qquad \text{and} \qquad a_i = b_i = -S\eta/(1 + S^2)$$

It should be noted that taking the above values for the a's and b's is completely equivalent to assuming that one solution for the potential $\Phi(\zeta)$ is that Φ is a constant.

3. Velocity Equation

Equ. (25) may be integrated to determine the velocity. The values of the a's and b's are substituted into Equ. (28) and that result substituted into Equ. (25), giving:

$$\frac{\epsilon k V_o^2}{2} \frac{\eta S \, e^{\frac{\eta(1-\zeta)}{1+S^2}} \left\{ \frac{1}{S} \sin\left(\frac{S\eta\zeta}{1+S^2}\right) + \cos\left(\frac{S\eta\zeta}{1+S^2}\right) - e^{-\frac{\eta\zeta}{(1+S^2)}} \right\}}{(1+S^2) \quad u(\zeta) \quad \left(\cosh\left(\frac{\eta}{1+S^2}\right) - \cos\left(\frac{S\eta}{1+S^2}\right)\right)} + \frac{C_1 d}{u(\zeta)} \tag{29}$$

For purposes of integration and evaluation the boundary conditions on the flow at $\zeta = 0$ and $\zeta = 1$, Equ. (29) may be written as:

$$\frac{\partial v_x}{\partial \zeta} = - D \frac{f(\zeta)}{u(\zeta)} + \frac{C_1 d}{u(\zeta)} \tag{30}$$

where:

$$D = \frac{\frac{\epsilon k V_o^2}{2} \eta S}{(1+S^2) \left(\cosh\left(\frac{\eta}{1+S^2}\right) - \cos\left(\frac{S\eta}{1+S^2}\right)\right)} \tag{31}$$

and:

$$f(\zeta) = e^{\frac{\eta(1-\zeta)}{1+S^2}} \left\{ - \frac{1}{S} \sin\left(\frac{S\eta\zeta}{1+S^2}\right) + \cos\left(\frac{S\eta\zeta}{1+S^2}\right) - e^{-\frac{\eta\zeta}{(1+S^2)}} \right\} \tag{32}$$

Integrating Equ. (30) gives:

$$v_x(\zeta) = -\int_0^{\zeta} D\,\frac{f(\zeta)\,d\zeta}{\mu(\zeta)} + \int_0^{\zeta} \frac{C_1\,d\,d\zeta}{\mu\,(\zeta)}$$

The boundary conditions for the flow are that at $\zeta = 0$ and $\zeta = 1$, the bottom and top of the channel, $v_x = 0$. In Chapter III it is shown that $\mu(\zeta) = \mu_o \zeta^{-4}$ where μ_o is a constant and this gives (when substituted in the above integrals):

$$v_x(\zeta) = -\int_0^{\zeta} \frac{D}{\mu_o}\, f(\zeta)\, \zeta^4\, d\zeta + \int_0^{\zeta} \frac{C_1 d}{\mu_o}\, \zeta^4\, d\zeta$$

which automatically satisfies the boundary condition at $\zeta = 0$. C_1 may be evaluated by satisfying the boundary condition at $\zeta = 1$. This leads to:

$$v_x(\zeta) = \frac{D}{\mu_o} - \left[\int_0^{\zeta} f\,(\zeta)\,\zeta^4 d\zeta + \zeta^5 \int_0^{1} f(\zeta)\,\zeta^4\,d\zeta\right] \qquad (33)$$

The velocity equation has several properties of interest, some are very interesting, in fact. First, it may be noted that the velocity is proportional to V_o^2 which appears in the constant D, and that when

$V_o = 0$ the velocity will be 0. This is the usual result in electric field problems of this sort. Second in the limit as $S \rightarrow 0$, which is the limit for 0 frequency $f(\zeta)$, goes to some constant value and $D \rightarrow 0$ so there can be no motion for 0 frequency. The limit for $\omega \rightarrow \infty$ may not be taken since it violates the conditions for which the equation was derived.

Surely the most interesting result of Equ. (33) concerns the dependence of v_x on η. The sign of η is determined by whether or not the conductivity gradient in the material from $\zeta = 0$ to $\zeta = 1$ is positive or negative. A positive gradient corresponds to $\eta > 0$ and a negative gradient corresponds to $\eta < 0$. In the expression for $f(\zeta)$, Equ. (32), if the sign of η changes, the only term which changes its sign is the sin term. When the expotential term $e^{\frac{-\eta S}{(1+S^2)}}$ dominates the expression in brackets in Equ. (32), as it will most of the time, a change in the sign of ζ will not change the sign of $f(\zeta)$. Therefore, the expression in brackets in Equ. (33) will not change sign. However, the constant D will change sign. That is, with a change in sign of the conductivity gradient, the pump may be made to move the fluid in a direction opposite to that of the traveling potential wave. This amounts to an inverse induction device. This direction reversal depends on the sign of the charge induced in the liquid. If the conductivity gradient is positive, that is the fluid is more conducting at the top than at the bottom, then

the charge induced in the liquid is positive. (Here we assume that E is negative,) The field is slightly ahead of the induced charge because of the charge relaxation in the liquid and the resulting electric force on the charges is opposite to the direction of travel of the field. If, on the other hand, the conductivity gradient is negative, then the charges induced are negative and the field tends to pull the charges in the direction of the field, dragging the fluid along with the charge.

The dependence of the sign of the charges on the sign of the conductivity gradient may be easily shown for the static case. Consider a liquid between two parallel plates with a voltage $+V_o$ applied across the plates from y = 0 to y = d, where y is the direction normal to the plates and a gradient in σ exists in the liquid such that $\sigma = \sigma_o + (\sigma_1/d)(y - y_o)$. In this case combining Equ. (2), (3) and (5) and noting that $\partial q/\partial t = 0$ for the static case it follows that:

$$q = \frac{\sigma_1}{\sigma_o} \frac{\epsilon E_o}{d} e^{\frac{-y}{d} \frac{\sigma_1}{\sigma_o}} \qquad (34)$$

where E_o is a constant determined by V_o. In this static case a positive gradient in σ corresponds to a positive charge, and changing the sign of of σ_1/σ_o changes the sign of the charge.

Even though at first glance a potential wave traveling in the +x direction inducing a fluid flow in the - direction may seem startling the theory predicts such a phenomenon and the static case would seem to

support this concept.

In Appendix A a dynamic problem with a singularity in conductivity gradient is done exactly and supports the conclusion of this theory.

CHAPTER III

FLUID PROPERTIES

A. Introduction

The liquid used in the electrohydrodynamic pump was AROCLOR 1232, manufactured by the Monsanto Chemical Company. The properties of the liquid which are of interest in the EHD pump experiment are the electrical conductivity σ, the dielectric constant, and the absolute viscosity μ. The value of the dielectric constant for AROCLOR was taken from the manufacturers published data*. The conductivity and the viscosity were determined by experiments.

B. Conductivity

Measurements of the conductivity of AROCLOR are not simple to perform in terms of repeatibility of data. The apparatus used in the experiments was relatively straight-forward, however. The conductivity was measured in a so called conductivity cell shown in Fig. 2. The cell consisted of a lower plate of aluminum, an upper plate of brass and pyrex walls. To measure the conductivity it was only necessary to place a sample of AROCLOR in the apparatus so that it completely filled the region between the plates.

---

* AROCLOR Platicizers, Monsanto Chemical Company, Technical Bulletin, No. PL - 306, p. 48.

A voltage was applied to the top plate. A 5 megohm resistor was connected between the bottom plate and ground and the voltage across this resistance was measured with a very high impedance (100 megohm) probe as shown in Fig. 3. Calling the value of the 5 megohm resistor R_r, the applied voltage V, the voltage measured across the resistor V_r, the separation of the plates d, and the area of the plates A, the conductivity σ was computed from the formula:

$$\sigma = \frac{d\ V_r}{A\ V\ R_r}$$

In order to determine the temperature dependence of the conductivity the apparatus described above was placed in a bath so that the level of the bath was above the level of the liquid inside the plates. For measurements above room temperature, this bath was mineral oil, heated with immersion resistance heaters. For measurements below room temperature, the bath was alcohol with dry ice. A thermometer was mounted in the apparatus so that the bulb was immersed in the AROCLOR. When the apparatus was placed in the cold bath frost tended to form on the sides of the pyrex shorting the top plate to the bottom plate. Consequently, the top was separated from the pyrex by blocks of plexiglass. This made the separation between the plates large enough for fringing fields to increase the effective area of the plates. This effect was corrected for by making measurements at room temperature with both the large and small separation,

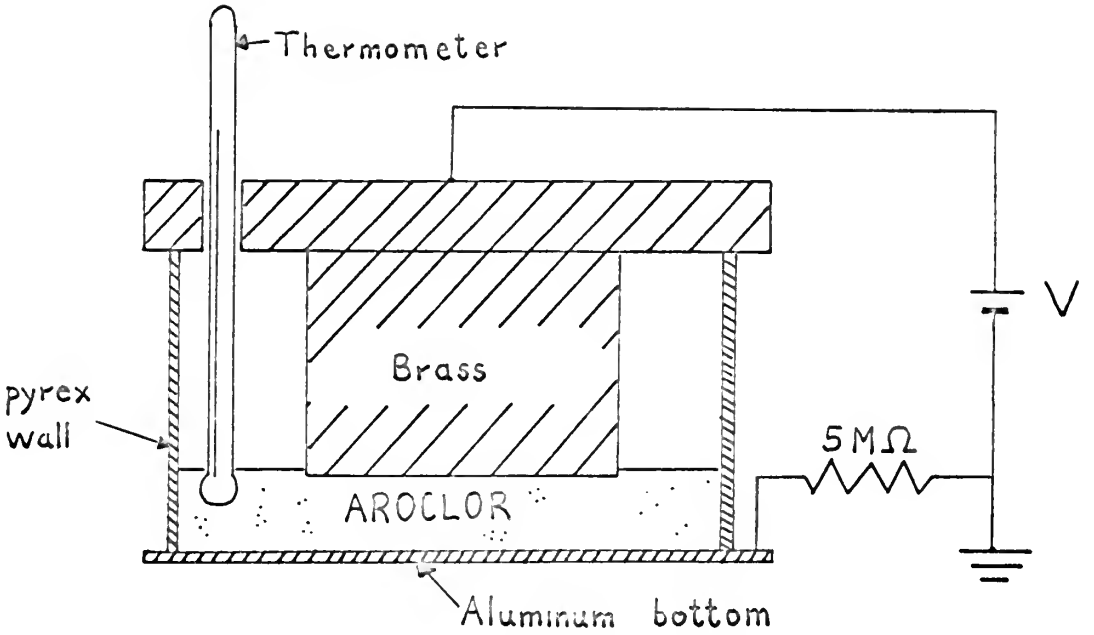

Figure 2 Conductivity cell for measuring conductivity of AROCLOR as a function of temperature.

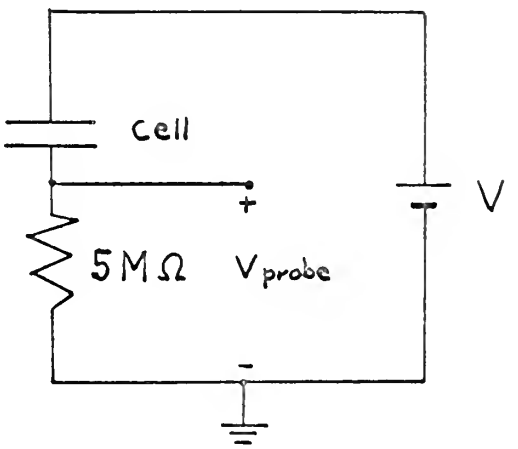

Figure 3 Conductivity cell circuit.

comparing the resulting values for σ and calculating a correction factor.

The results of the above experiment are shown in Fig. 4. These measurements were done at D.C. with a voltage applied of 6.0 kilovolts. The plate separation d was 2.15 cm, A was 33.6 sq. cm. and the correction factor for fringing was k = 0.815 in the formula $\sigma_{corrected} = k\,\sigma_{measured}$.

The nature of the actual mechanism for which electrical conductivity is a manifestation seems to be quite complicated in AROCLOR. By placing a point source of light in a position so that the light shines through the liquid and falls on a white screen, motion of the liquid may be easily observed. In an experiment performed with the conductivity cell described above with a temperature gradient applied across the cell, the motion of the liquid was observed as a function of applied voltage. In this experiment the temperature of the AROCLOR on the bottom was about $-25^{\circ}C$ and on the top about $+25^{\circ}C$. The plate separation was about 2 cm. for a gradient in temperature of $25^{\circ}C/cm$. With an applied voltage of less than 5 kilovolts at 1.5 cps. very little motion was observed. From 5 kilovolts to 7 kilovolts some local swirling of the liquid was noticed although it was not violent. At about 7 kilovolts a vaguely defined internal surface formed which undulated slowly. Above about 8

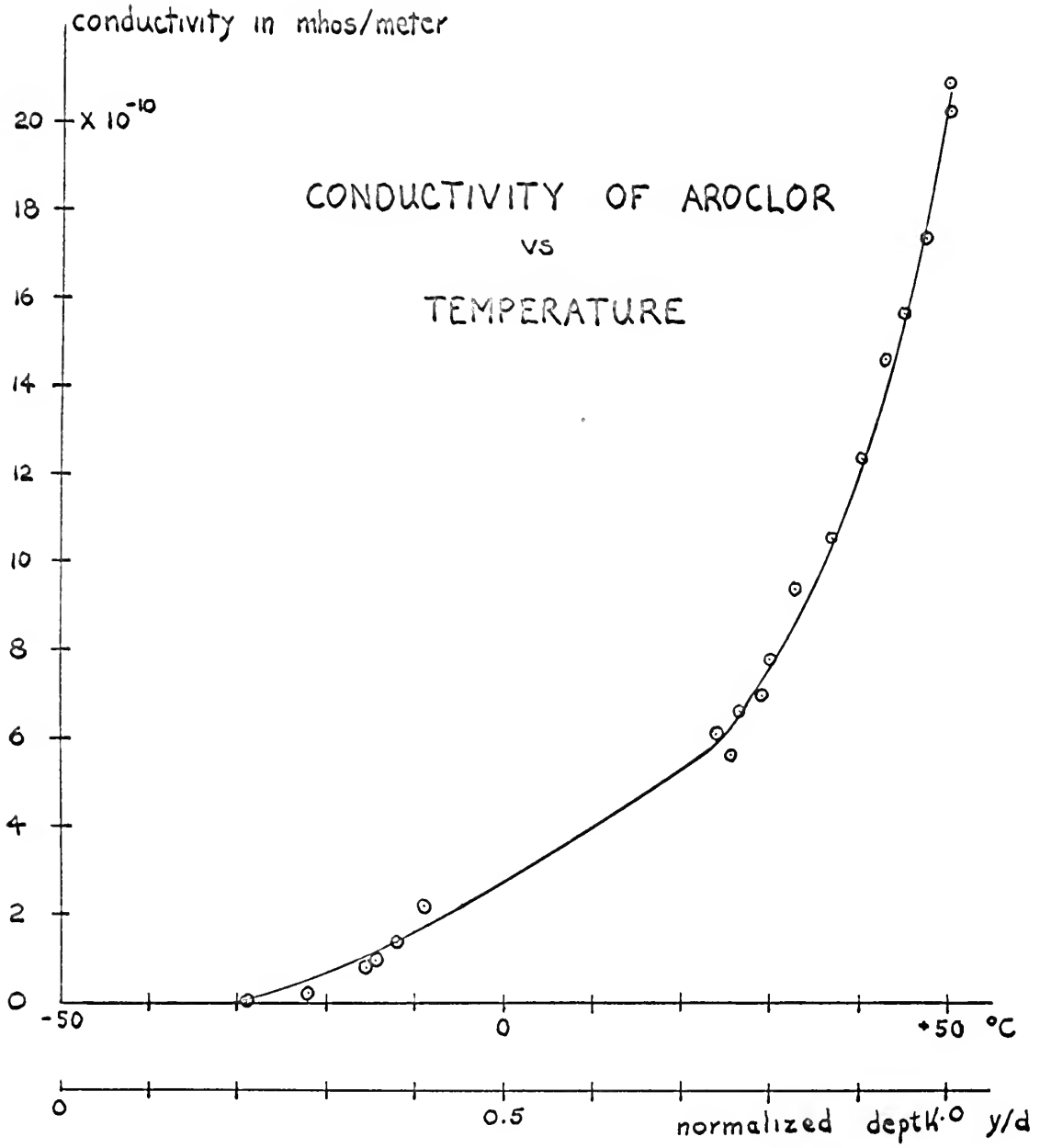

Figure 4 Results of measurement of conductivity of AROCLOR as a function of temperature for DC voltage of 6 kilovolts. Lower scale indicates conductivity as a function of normalized depth in pumping channel.

kilovolts this surface was completely eradicated by moderately violent swirling. Near 11 kilovolts the pattern of motion changes radically to very violent swirling. Under the conditions of this experiment gravity would tend to be stabilizing the liquid since the colder, denser material is on the bottom and the warmer,less dense material is on the top. However, the electric field is trying to leviate the material. Presumably, the electric field forces overbalance the gravitational force at some level of voltage and the fluid becomes unstable. This picture is complicated by the varying charge density within the material.

The result of the internal instabilities is to complicate understanding of the mechanism of conduction in the liquid. Mechanical motion of the liquid caused by the presence of the field, so-called electroconvection, may be very active in the process which results in current flow at the terminals of the conductivity cell.

In spite of the complexity of the mechanism for conduction in the AROCLOR, the data presented in Fig. 4 is assumed to represent the conductivity in the liquid as a function of temperature. The theory presented in Chapter II requires that σ be represented in the liquid as $\sigma = \sigma_o + \sigma_1 (\zeta - \zeta_o)$. As will be explained in Chapter IV, the temperature in the liquid in the pumping channel was assumed to be a linear function of the normalized distance ζ with the cold bottom corresponding

to $\zeta = 0$ and hot top corresponding to $\zeta = 1$.

Several approaches might be envisioned for approximating the data of Fig. 4 as $\sigma = \sigma_o + \sigma_1 (\zeta - \zeta_o)$. The first would be to say that σ_o is the mean value of σ and that σ_1 is the mean value of $d\sigma/d\zeta$. In that case, $\sigma_o = 10.5 \times 10^{-10}$ mho/meter and $\sigma_1 = 129 \times 10^{-10}$ mho/meter. ζ_o would then be 0.89. A second possibility would be to say that σ_o and σ_1 should be evaluated at $\zeta = 0.5$, that is, at the mid-depth of the channel. In that case $\sigma_o = 2.8 \times 10^{-10}$ mho/meter and $\sigma_1 = 11.2 \times 10^{-10}$ mho/meter. Of course, $\zeta_o = 0.5$. A third possibility would be to call σ_o the average value of σ and σ_1 the average value of $d\sigma/d\zeta$. In that event, $\sigma_o = 4.0 \times 10^{-10}$ mho/meter and $\sigma_1 = 20.3 \times 10^{-10}$ mho/meter. Then $\zeta_o = 0.6$. A final possibility exists which is influenced by the pumping theory and experiment. In Chapter V it is shown that the maximum pumping velocities attainable for a constant voltage occur at a frequency of 1.5 cps. In the theory of Chapter II the frequency dependence of velocity predicts that the maximum velocity is strongly influenced by the expression $\omega_\varepsilon/(\sigma_o^2 + (\omega_\varepsilon)^2)$, which has a maximum when $\sigma_o = \omega_\varepsilon$. For a frequency of 1.5 cps. this equation predicts that $\sigma_o = 4.75 \times 10^{-10}$ mho/meter which occurs at $\zeta_o = 0.66$. At that value of ζ_o $\sigma_1 = 11.2 \times 10^{-10}$ mho/meter. For calculations in this thesis, these latter values will be used. The other possibilities are presented to show the range of uncertainty which might

be expected as a result of the approximations made in the theory of Chapter II.

C. Viscosity

The viscosity of AROCLOR was measured using three Cannon-Fenske viscometers, ASTM Nos. 50, 200 and 400 to cover the temperature range of interest. The Cannon-Fenske viscometer measures ν, the kinematic viscosity*. Measurements were made over a range of temperature from $-5^{\circ}C$ to $68.75^{\circ}C$. The kinematic viscosity was converted to the absolute viscosity, μ, by the formula $\mu = \rho\nu$ where ρ is the density. The density of AROCLOR was taken from the manufactures data**. The results of the viscosity measurements are presented in Fig. 5. As with the conductivity measurements described earlier, the temperature was related to the normalized depth in the channel and the data of Fig. 5 was approximated by the analytic function $\mu = \mu_o \zeta^{-4}$ where $\mu_o = 5.7 \times 10^{-3}$ kg./m.-sec. This seems to be a very good approximation for the viscosity.

D. Dielectric Constant

As mentioned before the dielectric constant for AROCLOR was taken from the manufacturers data. The value used was 5.7 measured at 1000 cps.

*"Test for Kinematic Viscosity", (ASTM D445-IP 71)

**Op. Cit., Monsanto Technical Bulletin No. PL-306, pg. 41

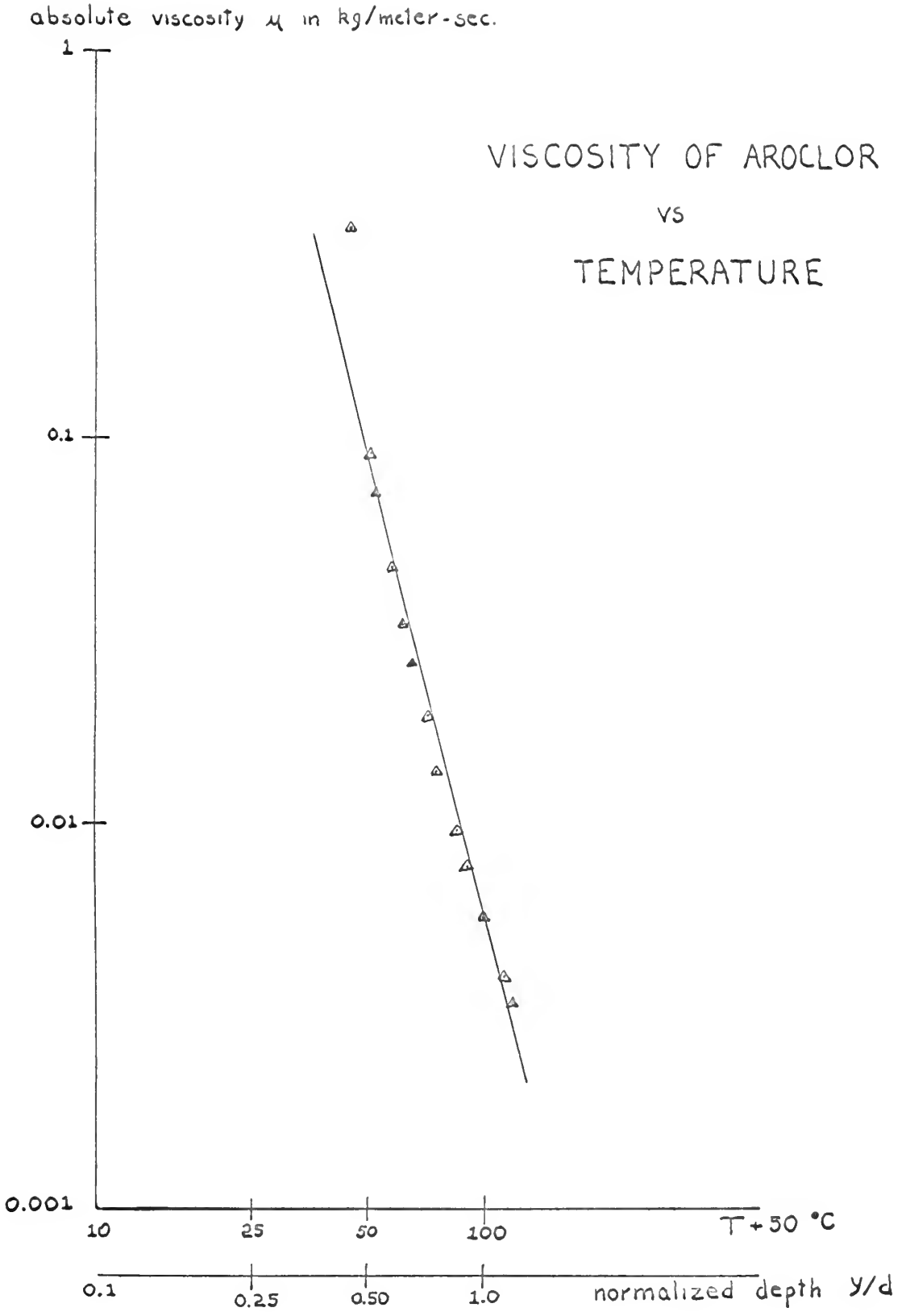

Figure 5 Results of measurement of absolute viscosity of AROCLOR as a function of temperature and normalized depth in pumping channel.

and 25°C. Since the pumping experiment was run at a mean temperature of 0°C and 1.5 cps. this value is only a approximation to that which existed in the pump. It is probable that the dielectric constant is also a function of frequency and temperature, however, this dependence was not measured and ϵ was assumed to be constant in the pumping experiment.

E. Conclusion

The values of the properties of AROCLOR used for calculation in this thesis are shown in Table 1. While the viscosity measurements were quite straight-forward and gave trustworthy results, the values for σ and ϵ are more open to question. Further experimentation with more careful measurement is indicated. There seem to be enough mysteries in the determination of the conductivity to justify a considerable expenditure of effort in careful experimentation.

PROPERTIES OF AROCLOR

absolute viscosity	$\mu = \mu_o \dot{\epsilon}^{-4}$	$\mu_o = 5.7 \times 10^{-3}$ kg/m-sec
conductivity	$\sigma = \sigma_o + \sigma_1 (\frac{y-y_2}{d})$	$\sigma_o = 4.75 \times 10^{-10}$ mho/meter $\sigma_1 = 11.2 \times 10^{-10}$ mho/meter
permittivity	ϵ = constant	$\epsilon = 5.7\ \epsilon_o$

Table 1 Properties of AROCLOR used in the evaluating of experimental results.

CHAPTER IV

THE EXPERIMENT

A. Introduction

The purpose of the experiment performed for this thesis was to demonstrate that slightly conducting liquids can be pumped according to the method purposed in Chapter I. Measurements were taken to determine how the velocity of the liquid in the flow depends on the voltage of the applied traveling potential wave, and how the velocity depends on the frequency of the applied traveling wave.

B. Apparatus

The apparatus used in the experiment is shown in Fig. 6. It is a modification of an apparatus used in an earlier experiment in EHD pumping of a liquid with a free surface. The liquid to be pumped was contained in a re-entrant, circular channel with insulating walls. made of plexiglass and a highly conducting bottom made of aluminum. The liquid was bound at the top of the channel by an arrangement of electrodes to which the traveling potential wave was applied. The dimensions of the channel were:

1) mean circumference 88.6 cm.
2) depth 4 cm.
3) width 5.1 cm.

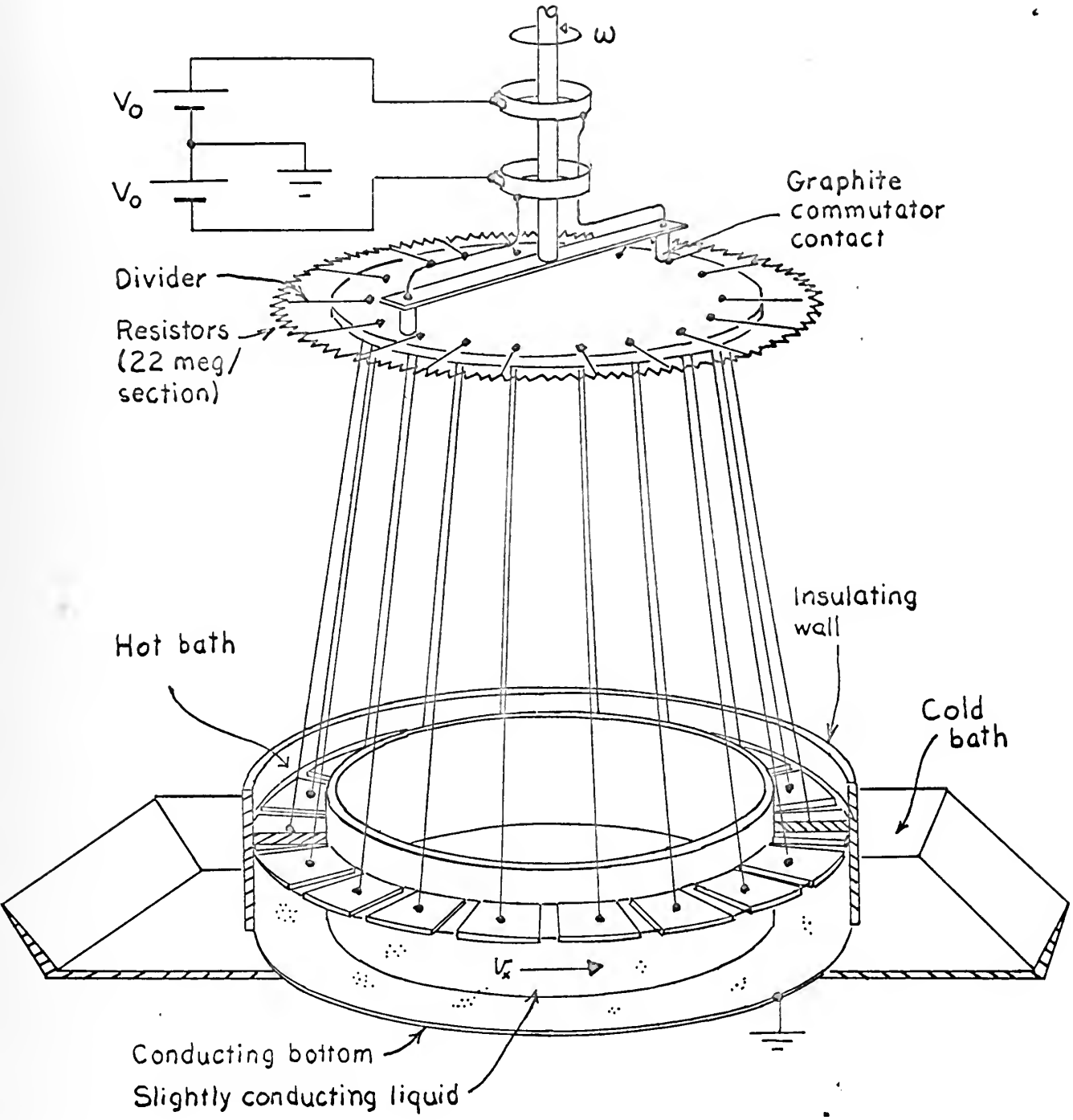

Figure 6 Apparatus used in the induction pumping experiment, showing traveling wave generator, pumping channel, and hot and cold baths.

The 40 electrodes which formed the top of the channel were individually connected to 40 contacts on a commutator ring. The 40 contacts were connected in a closed loop with a 22 megohm resistor connecting each two adjacent contacts. The commutator was a rotating plexiglass bar with a contact mounted at each end. One contact was connected through a slip ring to a potential of $+V_o$ volts and the other was connected through another slip ring to a potential of $-V_o$ volts. The commutator was rotated with an angular velocity ω. In this way, if the commutator was located at some particular angular position, ideally the potential on the electrodes varied linearly in small steps from $+V_o$ at one position at the top surface of the channel to $-V_o$ at the diametrically opposed position. Then as the commutator rotated the potential distribution moved around the channel as a traveling potential wave with a sawtooth shape. The actual wave which was created is shown in Fig. 7. The tendency of the wave shape to be more sharply peaked than an ideal sawtooth was caused by the loading effect on the power supplies of the liquid in the channel.

The liquid in the channel was AROCLOR 1232. Its properties have been described in Chapter III. The experiment requires that a gradient in electrical conductivity be established between the top and the bottom

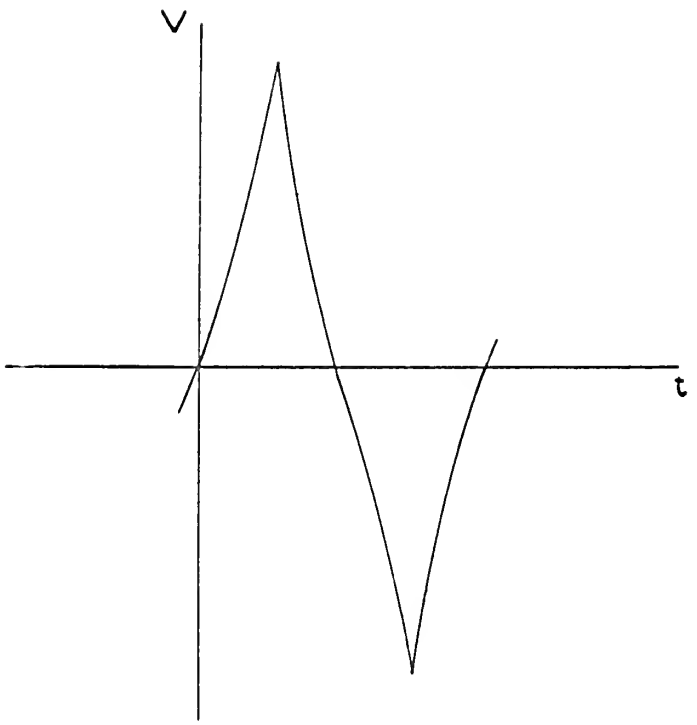

Figure 7 Approximate shape of voltage waveform produced by traveling wave generator. Fundemental component has a value of 0.66 V_o.

of the channel. To produce the required gradient advantage was taken of the fact that the electrical conductivity of AROCLOR is a function of temperature. Consequently, a temperature gradient was established in the liquid, between the top and the bottom of the channel. The bottom of the channel was put in contact with a bath of dry ice in alcohol which kept the bottom of the channel at a temperature of approximately -52°C. The region above the electrodes on the top surface was heated by circulating hot mineral oil in a channel above the electrodes. The mineral oil was physically separated from the AROCLOR by the plexiglass ring which also served as a mount for the electrodes. Heat from the circulating mineral oil was conducted to the AROCLOR by the electrode mounting bolts. The mineral oil was maintained at a temperature of approximately +62°C. By this method, a temperature difference of about 114°C was maintained between the top and the bottom of the channel. It should be noted, however, that the temperatures measured were the temperatures of the alcohol bath and the mineral oil and not the temperature of the AROCLOR at the top and bottom of the channel. While the heat conduction through the aluminum plate at the bottom was probably quite good, it is likely that heat conduction from the mineral oil to the AROCLOR was relatively poor. A reasonable assumption seems to be that the temperature at the top of the channel

was about +50°C and at the bottom, -50°C. This gives a total temperature difference of 100°C across the channel, or a temperature gradient of 25°C/cm. , assuming that the variation in temperature from the bottom ($\zeta = 0$) to the top ($\zeta = 1$) of the channel is linear. The measurement of the velocity of the fluid flow was done by suspending a few small particles of bakelite in the AROCLOR and measuring the time that a particle took to proceed around the channel. The particles stayed suspended in the liquid because a density gradient was caused by the gradient in temperature. The specific gravity of the bakelite particles was such that they would sit in the density gradient of the liquid. The progress of the particles around the channel was observed through the clear plexiglass walls. The particles were about 1/8 in. in diameter so that they were massive enough that even if they were themselves slightly charged, they would still respond to the fluid motion and not more independently of the fluid.

C. Procedure

Two interesting experiments were performed with the apparatus described above. The experiment to measure the dependence of the flow velocity on the voltage of the applied potential wave was done at a frequency of 1.5 cps. for a range of voltages between 7.0 kilovlots and 13.0 kilovolts in increments of .5 kilovolts. At each voltage the velocity of a particle in the flow was measured several times. At voltage levels below 7.0

kilovolts the particle velocities were quite small and somewhat difficult to measure. Since the electric field in addition to inducing a flow is also tending to leviate the liquid against the gravitational force. Above 13.0 kilovolts the liquid became so unstable internally that the flow was wiped out by the violent local motions of the liquid. The very unstable motion of the liquid was easily observable as swirls of liquid of slightly different refractive indices which could be seen in the presence of a strong light. This experiment was conducted at a frequency of 1.5 cps, since at a constant voltage, that frequency resulted in the largest velocities. Some variations in the velocities measured for a given set of conditions were observed and were caused by particles sitting at different places in the flow in both the vertical and the horizontal directions.

Repeatibility of data was difficult to attain unless the AROCLOR was allowed to remain in the channel for several hours before the experiment was performed. This may have been due to the fact that the AROCLOR was slightly corrosive to the plexiglass walls of the channel and some time was necessary to allow this process to achieve some equilibrium.

Another experiment was performed to find the dependence of velocity on the frequency of the applied traveling potential wave. This experiment was performed at a constant voltage of 10 kilovolts. This voltage level was chosen because the particle velocity was

relatively fast and allowed measurements to be made reasonably quickly but the liquid was still quite stable with regard to violent internal motions. The velocity of the flow was measured over a range of frequencies from about 0 cps. to 5.5 cps in intervals of about 0.5 cps. This range of frequency was used because of physical limitations imposed by the design of the commutator contacts.

In both of the experiments described here, the temperature gradient which was established across the channel was constant, so that the gradient in electrical conductivity was the same. Another experiment which would vary the gradient in conductivity could be envisioned but was not performed. The results of the experiments measuring velocity as a function of frequency and of voltage are shown in Figs. 8 and 9 in Chapter V.

CHAPTER V

RESULTS

A. Introduction

In this chapter the results of the experiment described in Chapter IV will be presented and discussed in relation to the predictions of the theory presented in Chapter II. A program for further experimentation will be introduced as well as some ideas for examining the theory pertinent to this area of EHD induction in the context of modifications to the experiments presented in this thesis.

B. Experimental Results

Figure 8 presents the results of the experiment which measured the velocity as a function of frequency. The data indicates that for 0 frequency the flow velocity is 0. This result is predicted by the theory. The data indicates that maximum v_x is achieved at a frequency of 1.5 cps.,and that v_x gradually decreases at higher frequency. The theory indicates that v_x is strongly dependent on the factor $\eta S/(1+S)^2$ which may be rewritten as $\sigma_1 \omega/(\omega_o^2 + (\omega_e)^2)$. Notice that there are also frequency terms in the expression for $f(\zeta)$ on frequency in this experiment will probably not, however, be as strong as the dependence on $\sigma_1 \omega_e/(\sigma_o^2 + (\omega_e)^2)$. A theoretical curve is plotted on the data in Fig. 8 showing the degree of similarity. The exact theoretical prediction of the frequency

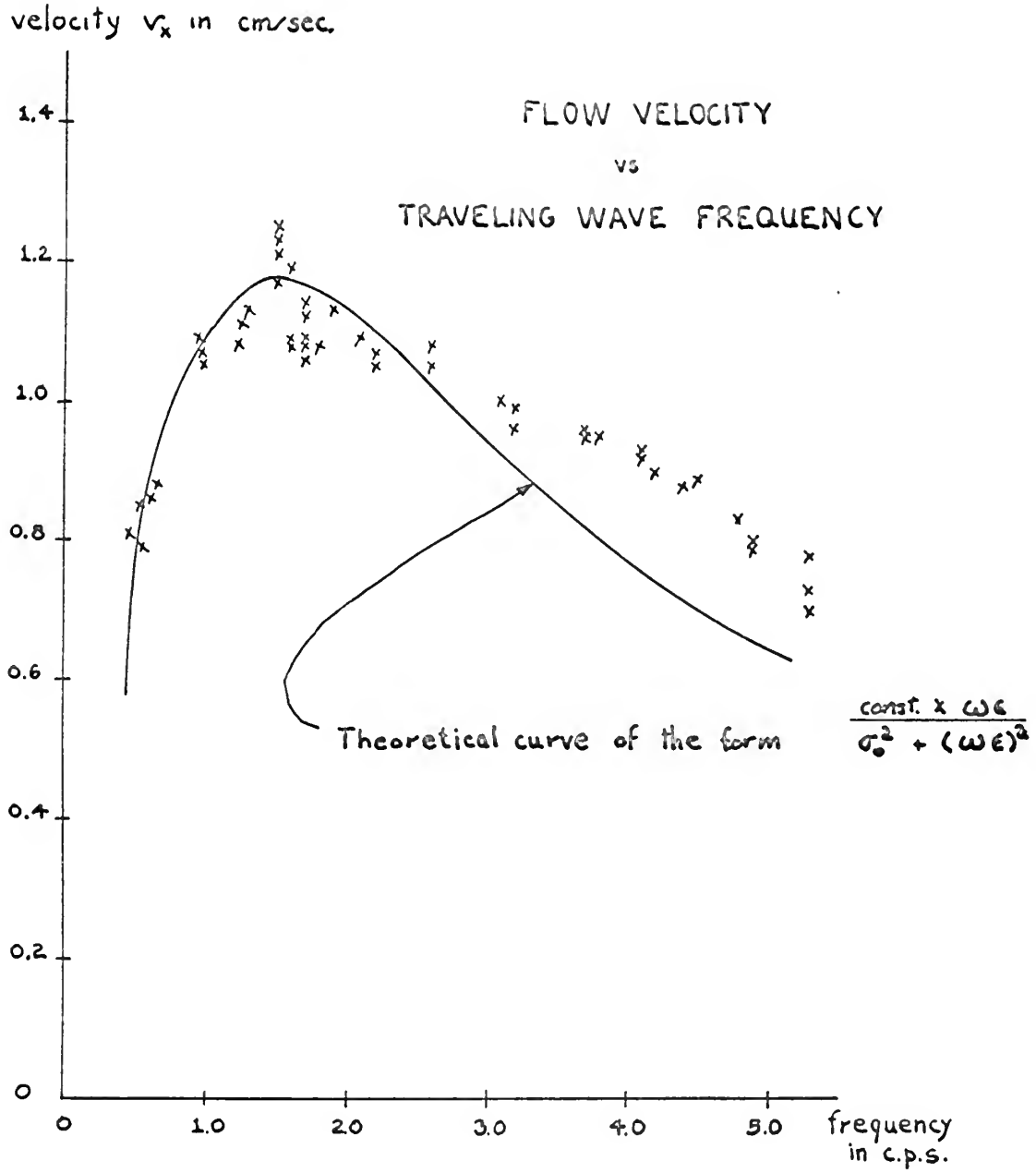

Figure 8. Results of experimental measurement of flow velocity as a function of frequency for V_o = 10.0 kilovolts with a 100°C ΔT between top and bottom of pumping channel.

dependence involves a computational problem of modest complexity which could be done easily on a digital computer but was not done for this thesis.

As mentioned in Chapter III, the existence of the peak in the data of Fig. 8 was used as a key to determining a likely value for σ_o. It is of interest that the value of σ_o predicted by this peak is within the range of values generated during the independent measurement of σ by the method of Chapter III.

Fig. 9 presents the results of the experiment which measured the velocity as a function of the voltage. These results are plotted against as V_o^2. The data clearly justifies the theoretical prediction that the velocity is linearly dependent on the voltage squared. The constant of proportionality which is the slope of the estimated line through the data points is 1.2×10^{-10} volt^2 sec/meter. This data could be plotted not against the peak voltage of the wave form shown in Fig. 7 . of Chapter IV, but instead against the peak value of the first fourier component of the voltage. The first fourier component has a peak of $0.66V_o$.* In this case the slope of the line of v_x versus $(0.66V_o)^2$ would be 2.75×10^{-10} volt^{2}sec/meter.

* Computed for the same wave shape by J.R. Melcher in "Traveling Wave Induced Electroconvection", to be published in Physics of Fluids.

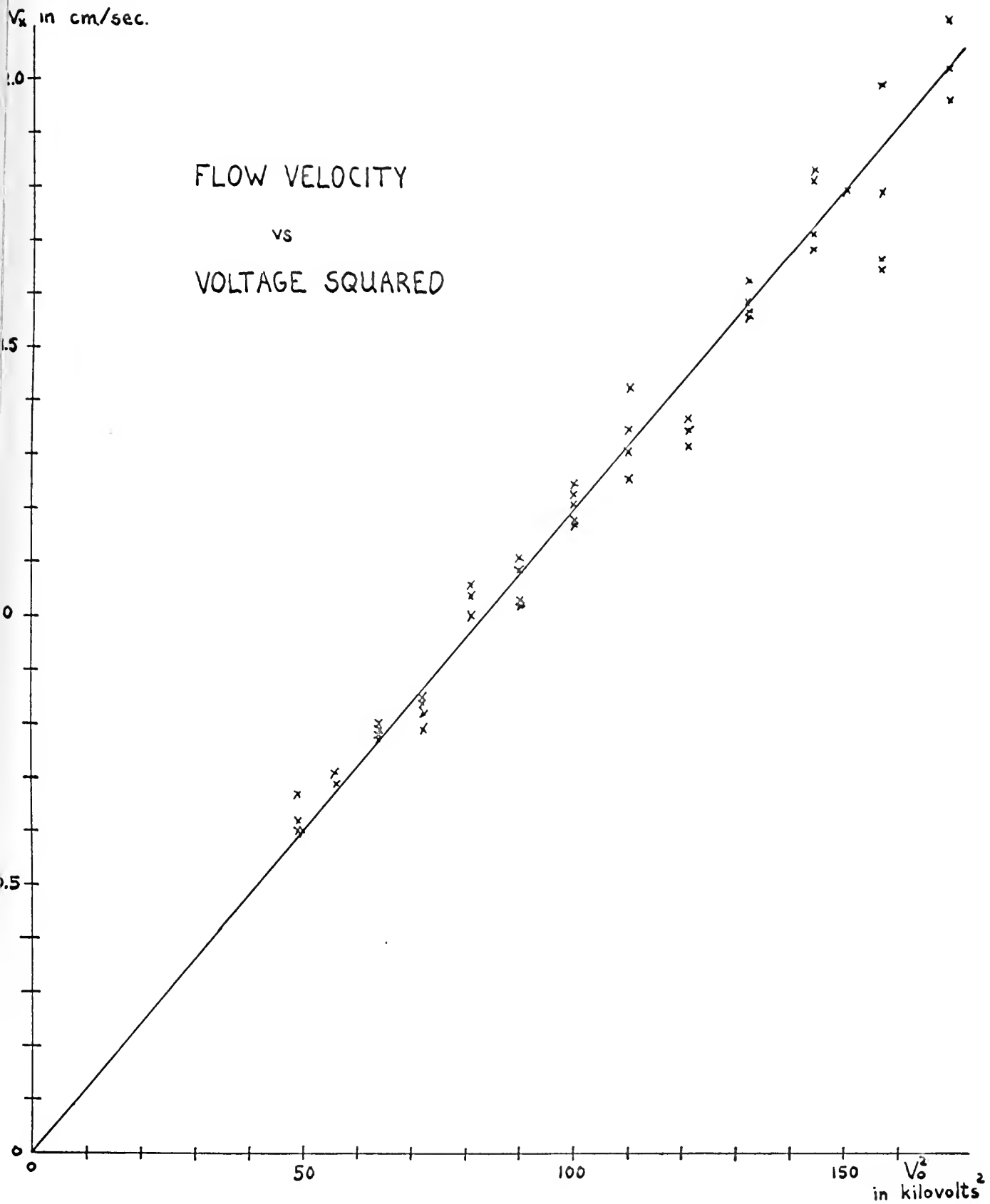

Figure 9. Results of experiment measurement of flow velocity as a function of traveling wave potential V_o. Plotted as velocity vs. voltage squared. Measurements made at a frequency of 1.5 c.p.s.

Turning now to the theory, the predicted slope of the line of v_x versus V_o^2 may be computed. Using the values for σ_o and σ_1 of Chapter III, the value of η is 2.36. The wave number k for this experiment is computed from $k = 2\pi/\lambda$ where λ, the wave length of the traveling wave, is the mean circumference of the channel. By this means k is determined to be 7.1 meters^{-1}. Since the data was taken at a frequency of 1.5 cps., which is the frequency for maximum v_x, $S = \omega\varepsilon/\sigma_o = 1$. With these values and the values for μ_o and ε from Chapter III, Equ. (33) may be numerically integrated. The value of ζ used for the integration is 0.7 which corresponds to the approximate position at which the particles used to measure the velocity were observed to float. Incidentally, some error is introduced here since particles often floated at varying depths but mostly with in a range of $\zeta = 0.5$ to $\zeta = 0.8$. In any case, performing the numerical integration for $\zeta = 0.7$ by Simpson's Rule gives that the slope of the line for v_x at $\zeta = .7$ versus V_o^2 should be $-1.17 \times 10^{-10} V_o^2$. Notice the minus sign. After all, the theory predicted that with a positive conductivity gradient, inducing a positive charge in the liquid, the flow should be in the direction opposite to the direction of travel of the traveling potential wave. The magnitude of the slope certainly agrees closely with the experiment. However, in the experiment the liquid proceeded in the wrong

direction, which at first glance is somewhat alarming.

The resolution of this discrepancy between the theory and the experiment may be found in a closer examination of the exact thermal conditions in the channel. Unfortunately, in the experiment as performed and described in Chapter IV, the measurement of the actual temperature profile in the liquid was never done. The thermal relaxation time for AROCLOR is approximately 2×10^3 seconds for distance on the order of 3 or 4 mm., which would be a reasonable dimension for the kinds of swirling motion observed in the liquid during various experiments. This long thermal relaxation time means that when the liquid in a temperature gradient is stirred, the gradient will not re-establish itself in the liquid for some considerable time. As mentioned in Chapter II, the electric field imposed on the liquid has a strong tendency to levitate the liquid against the force of gravity and make it internally unstable. It may be that the field induces charge in the liquid as expected by the positive gradient in σ and then the electric forces on this induced charge cause it to displace some of the warmer liquid near the top of the channel with cooler liquid from the bottom. Then, because of the long thermal relaxation time the original temperature gradient is not re-established. This is the same as saying that the internal instability of the liquid allows the formation of a temperature inversion layer. In this case, a region exists in the flow which has a negative conductivity gradient and

the induced motion of the liquid is in the positive direction, as the theory predicts. The liquid very near the top would still have a positive gradient in conductivity as well as that near the bottom. In the experiment performed, for the most part velocity measurements were only made in a range near the mid-depth of the channel. Besides, the very cold liquid near the bottom is quite viscous so that velocities there would be small in any case.

It is of great interest that the following observations were made during the experimentation. Early in the experiment process, before the theory had been fully developed, it was observed that in the presence of a gradient of about $30^{\circ}C$, where the liquid was only cooled on the bottom but was near room temperature at the top, the liquid was observed to flow very slowly in the direction opposite to that of the traveling wave. The velocities were small and it was thought that a larger temperature gradient would produce greater velocities. A larger gradient was applied and indeed larger velocities resulted and in the same direction as the traveling wave. Unfortunately, the author's intuition that the induced flow ought to be in the direction of the traveling wave, led him to continue working with the larger temperature gradient. No meaningful data was taken for the backward flow case.

During the measurement of v_x versus frequency some particles, which were floating just below the mid-depth of the channel, were observed to move

very slowly backward at the higher frequencies. This is another indication of the worth of the theory but this situation has not yet been pursued in detail.

C. Further Work

This experiment has shown that electroconvection can be induced. A theory now exists which correlates with the experiment in some ways. Further experiments are indicated, however. If the temperature gradient which actually exists in the liquid under the conditions described in Chapter IV were carefully measured, the results of this experiment could be better interpreted in relation to the theory.

Another experiment might be done to demonstrate the flow in the backward direction. The distribution of positive charge which results in the liquid with a positive conductivity gradient is different than the distribution of negative charge which results with a negative conductivity gradient. This may be seen in Equ. (34) of Chapter II. Therefore, if the sign of the conductivity gradient changes but the absolute magnitude remains the same, both the sign and the magnitude of the velocity will change. That is pumping backward is not exactly the reverse of pumping forward.

The most interesting extension of the theory which should be made is to do what might be called a multi-region analysis. This would only be a matter of considering the liquid in the channel sliced into different

regions. The conductivity approximation $\sigma = \sigma_o + \sigma_1(\zeta-\zeta_o)$ could be very accurate in each region. With proper sized slices σ_o would be sufficiently larger than σ_1 so the approximation in Equ.(9) that $\sigma = \sigma_o$ but $\nabla\sigma = \sigma_1$ would be very good. The appropriate boundary conditions would be to match fields and velocities at each interface between regions. This problem would require computer solutions.

The theory of Chapter II is the theory for the long wave limit which is the case for which the term $2dk \ll \eta/1 + jS$. The short wave limit which is the reverse inequality is presented in a very brief form in Appendix B. An experiment might also be performed where this limit is valid to test the theory through its entire scope.

Another major area of interest was mentioned briefly in Chapter III. The schemes discussed in this thesis for EHD induction pumping have possibilities as methods for further definition of the mechanism for conduction in liquids and for the investigation of electrically induced internal instabilities in liquids.

REFERENCES

1. Chandrasekhar, S., Hydrodynamics and Hydromagnetic Stability, London 1961.

2. Fano, R..M., Chu, L. J. and Adler, R. B., Electromagnetic Fields Energy and Forces, New York, 1960.

3. Melcher, J. R., "Traveling Wave Induced Electroconvection", to be published in Physics of Fluids.

4. Woodson and Melcher, Class notes for Fields, Forces, and Motions., M.I.T., Cambridge, Massachusetts, 1964.

5. Monsanto Chemical Company, "Aroclor Plasticizers", Technical Bulletin No. PL - 306, St. Louis, 1960.

6. 1965 Book of ASTM Standards, Part 17, Section (ASTM D 445 - IP 71), "Test for Kinematic Viscosity."

APPENDIX A

SOLUTION FOR A SINGULAR CONDUCTIVITY GRADIENT

A problem similar to the bulk EHD induction pump would be a pump operating with two liquids of differing σ's and ε's. Consider a device with the same electrical arrangement as that described in Chapter IV but with a liquid in the upper region of parameters σ_u and ε_u and a liquid in the lower region of σ_ℓ and ε_ℓ. (See Figure 10). In this case the induced charges will relax to the interface forming a sheet of charge at $y = 0$. Solving Maxwell's equations for the electric case will result in potential's in the two regions of the form:

$$\Phi = \text{Re}\left[A \sinh ky + B \cosh ky\right] e^{j(\omega t - kx)} \qquad (1)$$

the resulting field will be

$$\hat{E}_y = -k\left[A \cosh ky + B \sinh ky\right] \qquad (2)$$

$$\hat{E}_x = jk\left[A \sinh ky + B \cosh ky\right] \qquad (3)$$

The boundary conditions are:

at $y = a$ $\Phi = V$

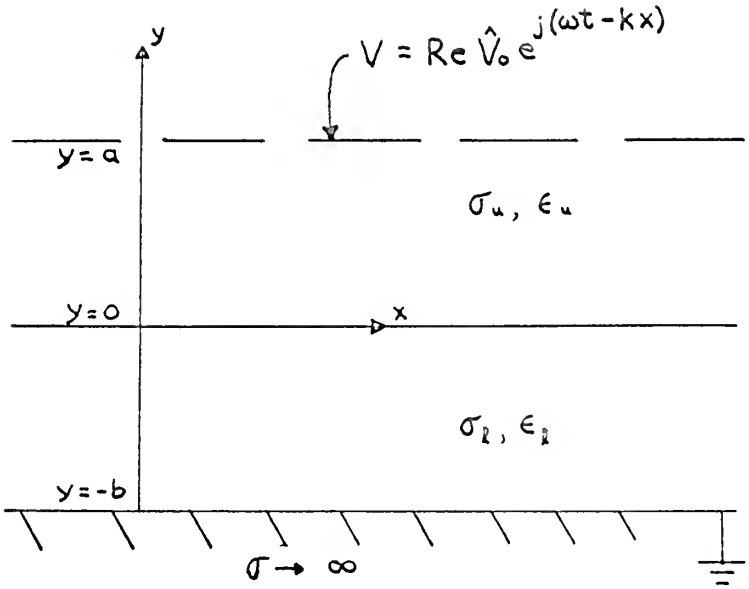

Figure 10. Coordinate system for the two fluid problem with a singularity in conductivity gradient at the interface.

at $y = 0$ $\quad Ex_u = Ex_\ell$ and

$$\sigma_u Ey_u - \sigma_\ell Ey_\ell + \frac{\partial}{\partial t}(\varepsilon_u Ey_u - \varepsilon_\ell Ey_\ell) + U\frac{\partial}{\partial x}(\varepsilon_u Ey_u - \varepsilon_\ell Ey_\ell) = 0$$

at $y = -b$ $\quad \Phi = 0$

where the u and ℓ indicate the upper and lower regions and U is the velocity in the x direction at the interface. Matching these conditions with the expressions for the potential and the fields in each region, equations (1), (2), and (3) gives:

$$V_o = A_u \sinh ka + B_u \cosh ka \tag{4}$$

$$0 = B_u - B_\ell \tag{5}$$

$$0 = (\sigma_u + j(\omega - kU)\varepsilon_u) A_u - (\sigma_\ell + j(\omega - kU)\varepsilon_\ell) A_\ell \tag{6}$$

$$0 = -A_\ell \sinh kb + B_\ell \cosh kb \tag{7}$$

The time-average electric traction at the surface will be given by the Electric Stress Tensor and will be:

$$< T_{xy} > = \mathrm{Re}\,\frac{1}{2}\left[\varepsilon_u \hat{Ey}_u \hat{Ex}_u^* - \varepsilon_\ell \hat{Ey}_\ell \hat{Ex}_\ell^*\right] \tag{8}$$

After solving for the A's and B's from equations (4) to (7), then combining equations (2) and (3) with (8), the time-average traction becomes:

$$\langle T_{xy} \rangle = \frac{k^2 V_o^2 (\cosh kb \sinh kb)\varepsilon_u(\omega-kU)(\sigma_\ell \varepsilon_u - \sigma_u \varepsilon_\ell)}{2\left[\sigma_u \cosh ka \sinh kb + \sigma_\ell \sinh ka \cosh kb\right]^2}$$

$$+ (\omega-kU)^2 \left[\varepsilon_\ell \sinh ka \cosh kb + \varepsilon_u \cosh ka \sinh kb\right]^2 \qquad (9)$$

If equation (9) is taken in the limit where $\sigma_u \to 0$ and $\varepsilon_u \to \varepsilon_o$, then the result is the same as that derived by Melcher for the single liquid with an air interface.* That is, for $\omega > kU$ the traction is positive. If, however, $\varepsilon_u = \varepsilon_\ell$ but $\sigma_u > \sigma_\ell$, conditions which would approximate those under which the experiment of this thesis was done, then the time-average electric traction is negative. In that case, U would surely be negative. The sign of the charge induced on the interface would be negative. Thus the result derived here for an exact solution agrees with the solution for the continuous gradient in conductivity of Chapter II.

---

*Melcher, op. cit.

APPENDIX B

Solution For Small Conductivity Gradient

From Equ. (28) of Chapter II a general expression for the time-average electric traction may be written in terms of the a's and b's, before taking the limit that $2dk \ll \eta/1+jS$. That expression is:

$$\langle T_{xy}^{E} \rangle = \frac{\epsilon k V_o^2 \, e^{-a_r(\zeta-1)} \, b_r \sin b_i\zeta - b_i \sinh b_r\zeta + a_i(\cosh b_r\zeta - \cos b_i\zeta)}{4d \qquad\qquad (\cosh b_r - \cos b_i)}$$

If instead of the above limit one takes the limit that $2dk \gg \eta/1+jS$ then the a's and b's are (from Equ. (26)):

$$a_r = b_i = 0; \quad b_r = 2dk; \qquad a_i = -\eta S/(1 + S^2)$$

Substituting these values into the above expression for T_{ij} gives:

$$\langle T_{xy}^{E} \rangle = - \frac{\epsilon k V_o^2 \, \eta S \, (\cosh 2dk\zeta - 1)}{4d \;\; (1+S^2) \;\; (\cosh 2dk - 1)}$$

Now if $2dk \ll 1$ this may be further approximated as:

$$\langle T_{xy}^{E} \rangle = - \frac{\epsilon k V_o^2 \;\; \eta S \zeta^2}{4d \qquad (1+S^2)}$$

With this new T_{ij}^{E} and $\mu = \mu_o \zeta^{-4}$ the velocity Equ.(30) may be integrated

to give:

$$v_x = \frac{\varepsilon k V_o^2 \eta S \zeta^7}{4\mu_o \, 1+S^2 \, 7} + \frac{C_1 d \zeta^5}{u_o \; 5} + C_2$$

When C_1 and C_2 are evaluated for the no-slip condition at $\zeta = 0$ and $\zeta = 1$ the result is:

$$v_x = \frac{\varepsilon k V_o^2 \eta S \zeta^5 (\zeta^2 - 1)}{28 \mu_o (1 + S)^2}$$

This equation for the limit of small conductivity gradient shows that in the limit where S becomes very large that the velocity $\rightarrow 0$ which means that the relaxation time is too long for the device to work at high frequencies. The equation also predicts that $v_x < 0$ for $\eta > 0$ and $v_x > 0$ for $\eta < 0$.